

## Journal Pre-proofs

Synthesis, molecular docking, dynamic simulations, kinetic mechanism, cytotoxicity evaluation of *N*-(substituted-phenyl)-4-{{4-[(*E*)-3-phenyl-2-propenyl]-1-piperazinyl} butanamides as tyrosinase and melanin inhibitors: *In vitro*, *in vivo* and *in silico* approaches

Hussain Raza, Muhammad Athar Abbasi, Aziz-ur-Rehman, Sabahat Zahra Siddiqui, Mubashir Hassan, Qamar Abbas, Hansol Hong, Syed Adnan Ali Shah, Muhammad Shahid, Sung-Yum Seo

PII: S0045-2068(19)31426-9  
DOI: <https://doi.org/10.1016/j.bioorg.2019.103445>  
Reference: YBIOO 103445

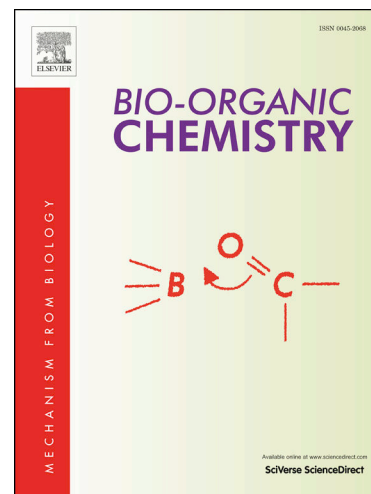
To appear in: *Bioorganic Chemistry*

Received Date: 30 August 2019  
Revised Date: 29 October 2019  
Accepted Date: 13 November 2019

Please cite this article as: H. Raza, M. Athar Abbasi, Aziz-ur-Rehman, S. Zahra Siddiqui, M. Hassan, Q. Abbas, H. Hong, S. Adnan Ali Shah, M. Shahid, S-Y. Seo, Synthesis, molecular docking, dynamic simulations, kinetic mechanism, cytotoxicity evaluation of *N*-(substituted-phenyl)-4-{{4-[(*E*)-3-phenyl-2-propenyl]-1-piperazinyl} butanamides as tyrosinase and melanin inhibitors: *In vitro*, *in vivo* and *in silico* approaches, *Bioorganic Chemistry* (2019), doi: <https://doi.org/10.1016/j.bioorg.2019.103445>

This is a PDF file of an article that has undergone enhancements after acceptance, such as the addition of a cover page and metadata, and formatting for readability, but it is not yet the definitive version of record. This version will undergo additional copyediting, typesetting and review before it is published in its final form, but we are providing this version to give early visibility of the article. Please note that, during the production process, errors may be discovered which could affect the content, and all legal disclaimers that apply to the journal pertain.

© 2019 Published by Elsevier Inc.



**Synthesis, molecular docking, dynamic simulations, kinetic mechanism, cytotoxicity evaluation of *N*-(substituted-phenyl)-4-{4-[(*E*)-3-phenyl-2-propenyl]-1-piperazinyl} butanamides as tyrosinase and melanin inhibitors: *In vitro*, *in vivo* and *in silico* approaches**

Hussain Raza<sup>a</sup>, Muhammad Athar Abbasi<sup>b,\*</sup>, Aziz-ur-Rehman<sup>b</sup>, Sabahat Zahra Siddiqui<sup>b</sup>, Mubashir Hassan<sup>c</sup>, Qamar Abbas<sup>d</sup>, Hansol Hong<sup>a</sup>, Syed Adnan Ali Shah<sup>e</sup>, Muhammad Shahid<sup>f</sup>, and Sung-Yum Seo<sup>a,\*</sup>

<sup>a</sup> *College of Natural Science, Department of Biological Sciences, Kongju National University, Gongju, 32588, South Korea.*

<sup>b</sup> *Department of Chemistry, Government College University, Lahore-54000, Pakistan.*

<sup>c</sup> *Institute of Molecular Biology and Biotechnology (IMBB), The University of Lahore, Lahore-54000,, Pakistan.*

<sup>d</sup> *Department of Physiology, University of Sindh, Jamshoro Pakistan.*

<sup>e</sup> *Faculty of Pharmacy and Atta-ur-Rahman Institute for Natural Products Discovery (AuRIns), Level 9, FF3, Universiti Teknologi MARA, Puncak Alam Campus, 42300 Bandar Puncak Alam, Selangor Darul Ehsan, Malaysia.*

<sup>f</sup> *Department of Biochemistry, University of Agriculture, Faisalabad-38040, Pakistan.*

---

**\*Corresponding Authors:** <sup>a</sup>Prof. Dr. Sung-Yum Seo, E-mail: [dnalove@kongju.ac.kr](mailto:dnalove@kongju.ac.kr) Tel: (+82)-416-8508503 and <sup>b</sup>Prof. Dr. Muhammad Athar Abbasi, E-mail: [abbasi@gcu.edu.pk](mailto:abbasi@gcu.edu.pk) Tel: (+92)-42-111000010 Ext. 266.

**Abstract**

In the current research work, different *N*-(substituted-phenyl)-4-{{4-[(*E*)-3-phenyl-2-propenyl]-1-piperaziny}}butanamides have been synthesized according to the protocol described in scheme 1. The synthesis was initiated by reacting various substituted anilines (**1a-e**) with 4-chlorobutanoyl chloride (**2**) in aqueous basic medium to give various electrophiles, 4-chloro-*N*-(substituted-phenyl)butanamides (**3a-e**). These electrophiles were then coupled with 1-[(*E*)-3-phenyl-2-propenyl]piperazine (**4**) in polar aprotic medium to attain the targeted *N*-(substituted-phenyl)-4-{{4-[(*E*)-3-phenyl-2-propenyl]-1-piperaziny}}butanamides (**5a-e**). The structures of all derivatives were identified and characterized by proton-nuclear magnetic resonance (<sup>1</sup>H-NMR), carbon-nuclear magnetic resonance (<sup>13</sup>C-NMR) and Infra-Red (IR) spectral data along with CHN analysis. The *in vitro* inhibitory potential of these butanamides was evaluated against Mushroom tyrosinase, whereby all compounds were found to be biologically active. Among them, **5b** exhibited highest inhibitory potential with IC<sub>50</sub> value of 0.013 ± 0.001 μM. The same compound **5b** was also assayed through *in vivo* approach, and it was explored that it significantly reduced the pigments in zebrafish. The *in silico* studies were also in agreement with aforesaid results. Moreover, these molecules were profiled for their cytotoxicity through hemolytic activity, and it was found that except **5e**, all other compounds showed minimal toxicity. The compound **5a** also exhibited comparable results. Hence, some of these compounds might be worthy candidates for the formulation and development of depigmentation drugs with minimum side effects.

**Keywords:** 1,4-Piperazine, butanamide, tyrosinase inhibitors, depigmentation, cytotoxicity.

## 1. Introduction

The biologically active nitrogen in piperazine ring and amide groups have a great importance in the therapeutical, pharmaceutical, material sciences, and pesticidal research fields [1]. Piperazine is an efficient functional moiety in biological and pharmacological investigations. It has represented its potential as anti-microbial [2], antiviral [3], anticoagulant, and anticancer agent [4]. It has also manifested insecticidal [5], herbicidal, and fungicidal potential [6] along with its plant growth regulator activity [7]. The various amide derivatives with heterocyclic rings showed excellent antibacterial *in vitro* and *in vivo* activity. The presence of lipophilic groups, like methoxy, methyls etc., enhanced the antimicrobial activity [8]. In order to enhance their therapeutic potential, the various other small functional groups have also been introduced in these derivatives [8]. Therefore, a large number of derivatives containing heterocyclic piperazine ring and amide groups have been synthesized which showed a large number of biological activities [9]. Animals, microorganisms and plants distributed copper bound enzyme known as tyrosinase. In plants and many organisms its reaction sequences monophenols to *o*-diphenols and oxidation reaction of *ortho*-diphenols to *ortho*-quinones. The tyrosinase enzyme is responsible for the alteration of texture, test and nutritional requirements of vegetables and fruits. In higher animals, humans and fungi this enzyme speeds up the transformation of tyrosine into melanin. Melanin is a pigment which is accountable for skin color and acts as a defense against ultraviolet radiations [10]. The elevated level of melanin pigment production is accountable for various skin disorders in females and males such as dark color, acne, melasma and ephelides. Therefore these type of studies encouraged scientists and researchers to synthesize the bioactive inhibitors of tyrosinase for the development of depigmentation drugs [11].

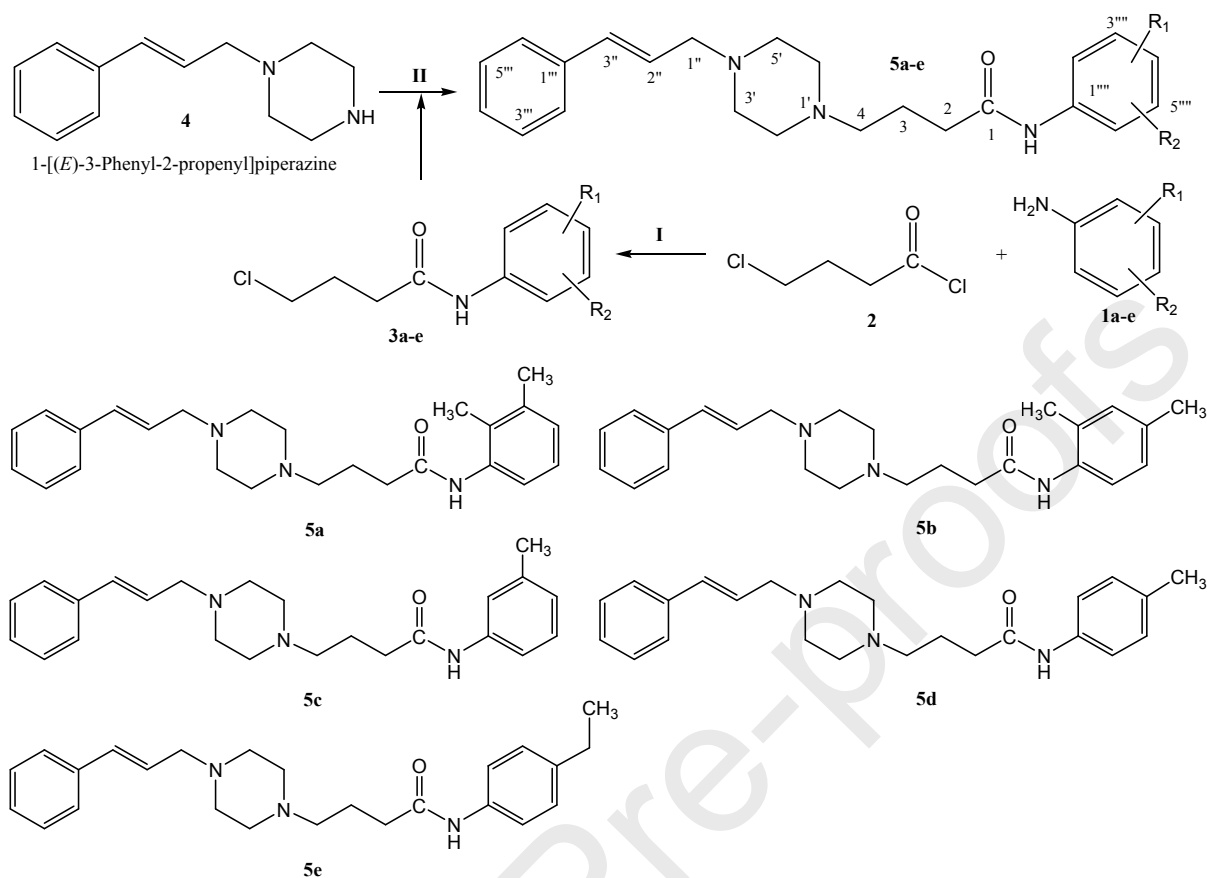
In the literature some piperazine or amide containing molecules have been reported as effective tyrosinase inhibitors [12-14], so the rationale in the present study was to synthesize some hybrid compounds bearing piperazine and butanamide moieties together in the same skeleton in order to explore their accumulative therapeutic effect for searching some new drug candidates for skin disorders.

## 2. Results and Discussion

## 2.1. Chemistry

A unique series of piperazine bearing butanamides (**5a-e**) was synthesized according to a protocol outlined in Scheme 1. The procedures of synthesis and conditions of reactions are described in the experimental section. The synthesis of targeted compounds was initiated by reacting substituted anilines (**1a-e**) with 4-chlorobutanoyl chloride (**2**) in the presence of aqueous alkaline medium under 4-5 hours stirring at room temperature to acquire the respective electrophiles, 4-chloro-*N*-(substituted-phenyl)butanamides (**3a-e**), in amorphous powder forms with different colors. Then, these electrophiles (**3a-e**) were coupled, one by one, with a nucleophilic 1-[(*E*)-3-phenyl-2-propenyl]piperazine (**4**) in the presence of acetonitrile and K<sub>2</sub>CO<sub>3</sub> by refluxing the mixture for 4-5 hours. In this way, the targeted compounds, *N*-(substituted-phenyl)-4-{4-[(*E*)-3-phenyl-2-propenyl]-1-piperazinyl}butanamides (**5a-e**), were obtained in good yields. The structures of these compounds were identified by using IR, <sup>1</sup>H-NMR, and <sup>13</sup>C-NMR spectral data along with CHN analysis data. The structural assignment of one of the compounds (**5a-e**) is described hereby for clear understanding of interpretational decorum of the synthesized compounds. The molecule **5e**, was obtained as light pink amorphous powder in 71% yield with a melting point of 125-126 °C. The molecular formula, C<sub>25</sub>H<sub>33</sub>N<sub>3</sub>O, of this compound was predicted with its CHN analysis data. Counting the number of protons in <sup>1</sup>H-NMR spectrum and carbon resonances in its <sup>13</sup>C-NMR spectrum was also in agreement with the deduced molecular formula. The speculated functionalities present in this molecule were affirmed by various vibrational bands in IR spectrum, at  $\nu$  3243 (N-H, str.), 3047 (Ar C-H, str.), 1711 (C=O, str.), 1635 (Ar C=C, str.), and 1592 (C=C, str.) cm<sup>-1</sup>. In its <sup>1</sup>H-NMR spectrum, (Figure 1a), the most deshielded singlet at  $\delta$  9.23 was rational for *N*-arylated amidic proton (Ar-NH-CO). A cinnamyl [(*E*)-3-phenyl-2-propenyl] moiety was depicted by two resonances, integrated for five protons of phenyl group, in aromatic region (Figure 1b) appearing at  $\delta$  7.44 (br.d,  $J$  = 7.5 Hz, 2H, H-2''' & H-6'''), and 7.33-7.31 (m, 3H, H-3''', H-4''', & H-5''') along three typical signals of (*E*)-2-propenyl moiety at  $\delta$  6.53 (br.d,  $J$  = 15.9 Hz, 1H, H-3''), 6.29 (td,  $J$  = 6.6, 15.9 Hz, 1H, H-2''), and 3.09 (br.d,  $J$  = 6.3 Hz, 2H, CH<sub>2</sub>-1''). The 4-ethylphenyl ring attached with nitrogen of acetamido group was represented by a peculiar A<sub>2</sub>B<sub>2</sub> spin system in aromatic region, signified by two *ortho*-coupled doublets at  $\delta$  7.22 (br.d,  $J$  = 8.0 Hz, 2H, H-2'''' & H-6'''), and 7.12 (br.d,  $J$  = 8.0 Hz, 2H, H-3'''' & H-5''') along with symbolic signals for an ethyl group in aliphatic region at  $\delta$  2.58 (q,  $J$  = 7.5 Hz, 2H, 4''''-CH<sub>2</sub>CH<sub>3</sub>), and 1.11 (t,  $J$  = 7.5 Hz, 3H, 4''''-CH<sub>2</sub>CH<sub>3</sub>). The proton signals of symmetrical

1,4-piperazine heterocycle and one other methylene group were merged and identified through two resonances at  $\delta$  3.38-3.34 (m, 4H, CH<sub>2</sub>-3' & CH<sub>2</sub>-5'), and 2.33-2.25 (m, 6H, CH<sub>2</sub>-2, CH<sub>2</sub>-2' & CH<sub>2</sub>-6'). The connecting butanamide moiety was characterized by typical peaks in aliphatic region at  $\delta$  2.48-2.47 (m, 2H, CH<sub>2</sub>-4), and 1.74 (quint.  $J = 7.1$  Hz, 2H, CH<sub>2</sub>-3) while the signal of a methylene (CH<sub>2</sub>-2) was intermixed with those of piperazine heterocycle as a multiplet, as mentioned above. All these assignments were verified with its <sup>13</sup>C-NMR spectrum, in which the (*E*)-3-phenyl-2-propenyl moiety was embodied by four signals of phenyl ring at  $\delta$  137.16 (C-1'''), 129.01 (C-3''' & C-5'''), 127.65 (C-4'''), and 126.58 (C-2''' & C-6'''), in addition to three signals for a 2-propenyl unit at  $\delta$  132.36 (C-2''), 126.25 (C-3''), and 60.65 (C-1''). 4-Ethylphenyl ring attached with nitrogen of amido group was deduced by resonances at  $\delta$  138.42 (C-1''''), 136.26 (C-4''''), 128.86 (C-3'''' & C-5''') for a phenyl ring while 4-ethyl moiety was depicted by two signals at  $\delta$  24.23 (4''''-CH<sub>2</sub>CH<sub>3</sub>), and 14.68 (4''''-CH<sub>2</sub>CH<sub>3</sub>). Four methylenes of a symmetrical 1,4-piperazine ring were unified by two signals at  $\delta$  53.29 (C-3' & C-5') and 53.20 (C-2', & C-6') [15]. The linking butanamido entity was specified by a downfield amidic carbonyl carbon at  $\delta$  171.76 (NH-CO) along with three methylene resonances at  $\delta$  57.81 (C-4), 34.17 (C-2), and 23.01 (C-3). Based upon, these cumulative evidences, the structure of **5e** was confirmed and named as *N*-(4-ethylphenyl)-4-{{4-[(*E*)-3-phenyl-2-propenyl]-1-piperazinyl}butanamide. A similar strategy was followed for structural interpretation of other butamides in the series. The <sup>1</sup>H-NMR and <sup>13</sup>C-NMR spectra of all compounds are shown in Fig. S5-S14.



**Scheme 1.** Outline for the synthesis of *N*-(substituted-phenyl)-4-{(4-[(*E*)-3-phenyl-2-propenyl]-1-piperazinyl}butanamides. **Reagents & Conditions:** (I) Aq. Na<sub>2</sub>CO<sub>3</sub> soln./pH 9-10/stirring at RT for 4-5 hrs. (II) Acetonitrile/K<sub>2</sub>CO<sub>3</sub>/refluxing of **4** for 0.5 hrs for its activation, followed by addition of respective electrophile, **3a-3e**, and then refluxing for 4-5 hrs.

## 2.2. Biology

### 2.2.1. Enzyme inhibition and structure-activity relationship

The synthesized compounds (**5a-5e**) were screened to corroborate their significance as tyrosinase enzyme inhibitors. The standard compound used for the screening was kojic acid and the evaluations of half-maximal inhibitory concentration (IC<sub>50</sub>) are summarized in Table 1. Interestingly, all synthesized compounds showed potent inhibition towards mushroom tyrosinase. Compared to kojic acid, the compound **5b** (0.013 ± 0.001) was dominant tyrosinase inhibitors as compared to other analogs in the series. The presence of two methyl groups at 1 and 4 positions in *N*-aryl moiety greatly affected the tyrosinase inhibition. The less sterically hindered substituents at these positions in *N*-aryl part probably made this molecule prone to interact strongly and occupy the pocket of the receptor in a superb manner. The compound **5a** was identified as the second most

potent inhibitor. Again it was attributed with similar two methyl groups but at 2 and 3 positions in the *N*-aryl part, however, this substitution pattern of methyl groups resulted in a very little decrease in the inhibitory effect, presumably due to the close proximity of these groups. The compound **5e** exhibited the least inhibitory potential comparatively in the synthetic series, probably due to relatively bulky ethyl group in it.

**Table 1**

IC<sub>50</sub> values of compounds (**5a-5e**) were calculated by nonlinear regression using GraphPad Prism 5.0.

Compound	Tyrosinase activity IC <sub>50</sub> ± SEM (μM)	Compound	Tyrosinase activity IC <sub>50</sub> ± SEM (μM)
<b>5a</b>	0.019 ± 0.013	<b>5d</b>	0.051 ± 0.037
<b>5b</b>	0.013 ± 0.001	<b>5e</b>	0.682 ± 0.112
<b>5c</b>	0.039 ± 0.006	Kojic Acid	16.841 ± 1.146

### 2.2.2. Kinetic analysis

Depending on our results, the most potent compound **5b** was selected to determine the inhibition type and inhibition constant on tyrosinase. The potential of this compound to inhibit free enzyme and enzyme-substrate complex was determined in terms of EI and ESI constants respectively. The kinetic studies of the enzyme by the Lineweaver-Burk plot of 1/V versus 1/[S] in the presence of different compound's concentrations gave a series of straight lines (Fig. 1A). The results of **5b** showed that the compound intersected within the second quadrant. The analysis showed that V<sub>max</sub> decreased with new increasing doses of inhibitors while K<sub>m</sub> remains the same. This behavior indicates that **5b** inhibit the tyrosinase non-competitively to form the enzyme-inhibitor complex. The Secondary plot of slope against the concentration of inhibitors showed enzyme inhibitor dissociation constant (K<sub>i</sub>) (Fig. 1B).

The kinetic results are presented in the Table 2. (Kinetic parameter table).

**Table 2**

Kinetic parameters of the mushroom tyrosinase for L-DOPA activity in the presence of various concentration of **5b**.

Concentration ( $\mu\text{M}$ )	$V_{\max}$ ( $\Delta\text{A}/\text{Sec}$ )	$K_m$ ( $\text{mM}$ )	Inhibition Type	$K_i$ ( $\mu\text{M}$ )
0.00	$9.16 \times 10^{-5}$	0.4	Non-Competitive	0.017
0.007	$4.07 \times 10^{-5}$	0.4		
0.013	$2.92 \times 10^{-5}$	0.4		
0.026	$2.45 \times 10^{-5}$	0.4		

$V_{\max}$  is the reaction velocity,  $K_m$  is the Michaelis-Menten constant,  $K_i$  is the EI dissociation constant.

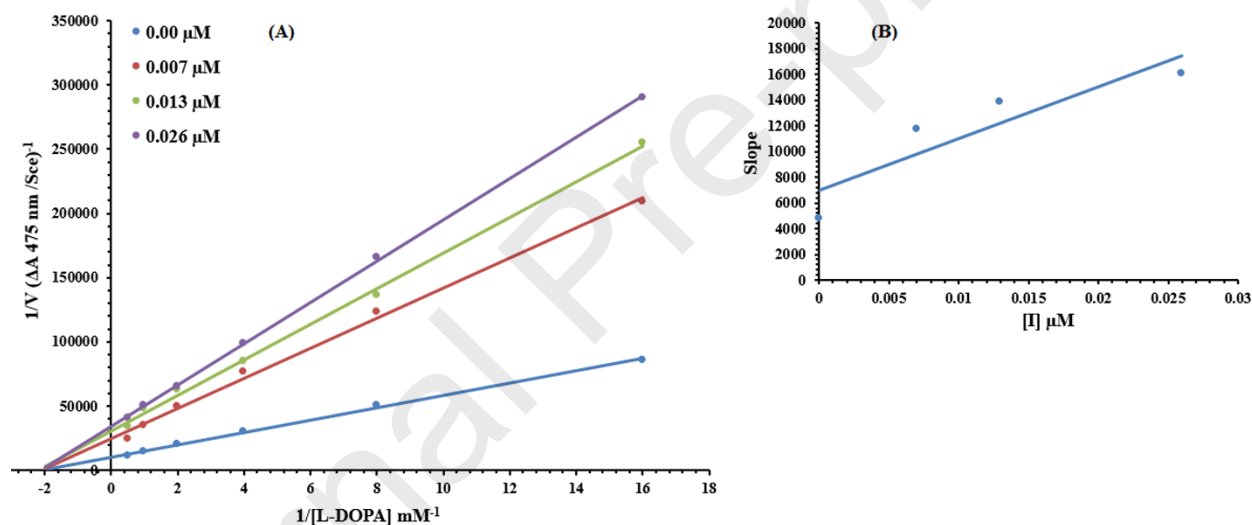


**Fig 1.** Lineweaver–Burk plots for inhibition of tyrosinase in the presence of Compound **5b**. (A) Concentrations of **5b** were 0.00, 0.007, 0.013 and 0.026  $\mu\text{M}$ , respectively. Substrate L-DOPA Concentrations were 0.0625, 0.125, 0.25, 0.5, 1 and 2  $\text{mM}$ , respectively. (B) The insets represent the plot of the slope versus inhibitor **5b** concentrations to determine inhibition constant. The lines were drawn using linear least squares fit.

### 2.2.3. Cytotoxicity

The cytotoxic potential of all synthesized compounds, **5a-e**, was evaluated through hemolytic assay. The percentage of cell hemolysis values of all synthesized compounds are given in Table 3. It is evident from the results that all compounds exhibited little toxicity towards red

blood cell membranes, compound **5e** showed little bit higher hemolysis activity ( $33.38 \pm 0.07\%$ ), as compared to other compounds, but it was much less than the positive control, (Triton-X) having a value of  $99.56 \pm 0.02\%$ . So, in general, all of these compounds can be regarded as harmless therapeutic agents.

**Table 3**

Cytotoxicity studies of the synthesized amides, **5a-e**.

Compound	% Hemolysis	Compound	% Hemolysis
<b>5a</b>	$6.73 \pm 0.05$	<b>5d</b>	$5.42 \pm 0.04$
<b>5b</b>	$3.94 \pm 0.03$	<b>5e</b>	$33.38 \pm 0.07$
<b>5c</b>	$0.58 \pm 0.01$	Triton X	$99.56 \pm 0.02$
Note: PBS (% Hemolysis) = $1.03 \pm 0.01$ .			

#### 2.2.4. *In vivo* depigmentation zebrafish assay

Zebrafish is a vital research model against various diseases, due to gene makeup similarity with human [11]. Owing to these benefits, the zebrafish seeds were used to determine the depigmentation efficacy of **5b** through *in vivo* assay. The inhibition efficacy of **5b** on the coloring of zebrafish was investigated with the treatment of 5, 10, 20 and 40  $\mu\text{M}$  of inhibitor **5b** and equal doses were tested for kojic acid. The pigment level of zebrafish significantly decreased  $P < 0.05$ , (Fig. 2) to about 53.55% while positive control kojic acid showed 25.53% at 40  $\mu\text{M}$ . Additionally, inhibitor **5b** exhibited good depigmenting effects at 20  $\mu\text{M}$  treatment, relative to those of kojic acid.

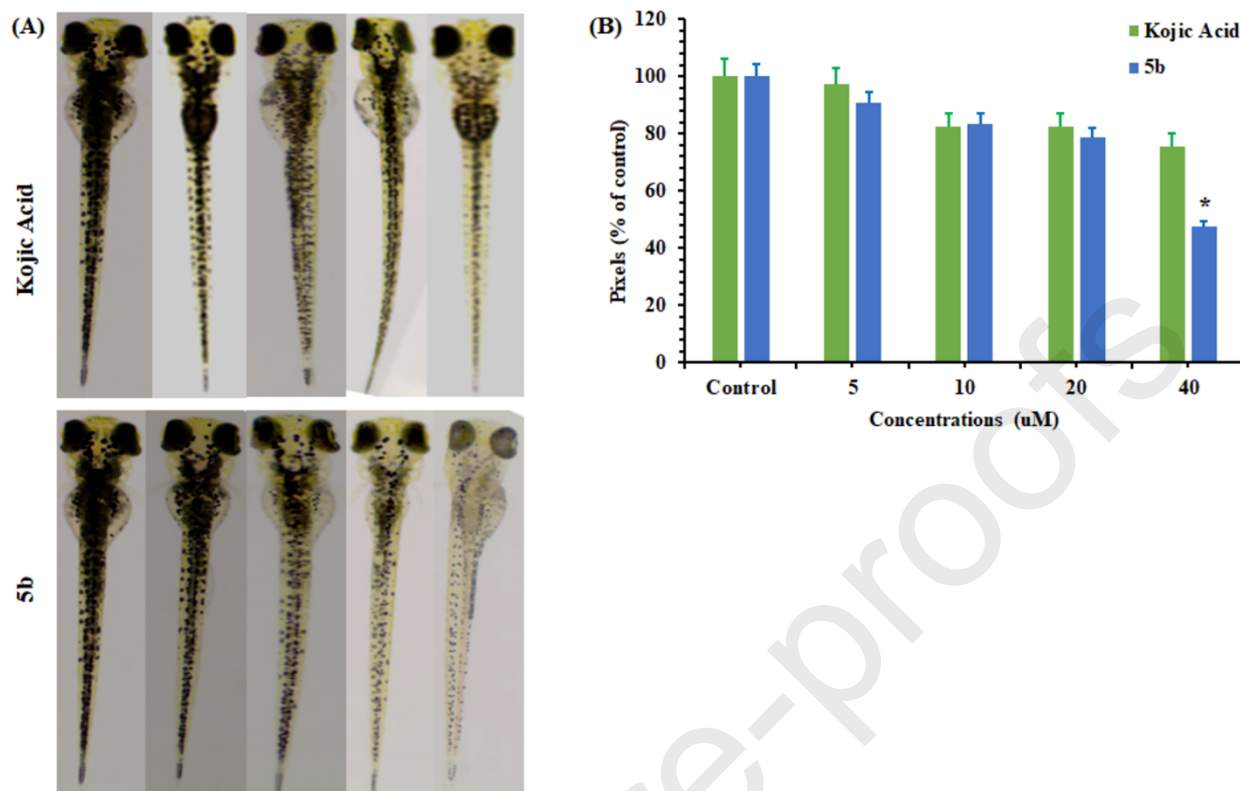


**Fig 2.** Depigmentation efficacy of **5b** in zebrafish (A) showed the rapid decrease in fish coloring from black brown to whitish at various doses (B) Pixel comparison of the depigmenting potency of **5b** and kojic acid. The fish image color intensity was measured using Image J software and compared using the t-test. \*P <0.05.

### 2.2.5. Molecular docking analysis

#### 2.2.5.1. Binding energy evaluation of synthesized compounds

To predict the best-fitted conformational position of synthesized ligands (**5a-e**) within the active region of the target protein. The generated docked complexes were analyzed based on Glide docking energy values (kcal/mol) and bonding interaction (hydrogen/hydrophobic) behavior. The lowest binding energy value depicts the best conformational position of the ligand within the active region of the target protein. The docking results showed that all the synthesized ligands (**5a-e**) bound within the active site of the target protein with different conformational poses and energy values, respectively. The binding pattern of all synthesized compounds showed their similar conformational behavior within the active region of the target protein (Fig. 3). The compound **5a** exhibited -6.34 (kcal/mol), whereas, **5b**, **5c**, **5d** and **5e** possessed -6.20, -5.32, 4.90 and 6.23 kcal/mol, respectively (Fig. 4). The comparative results showed that compounds exhibited good

docking energy values. The basic skeleton of all the synthesized compounds was similar therefore, no big energy value difference was observed in all docking results.

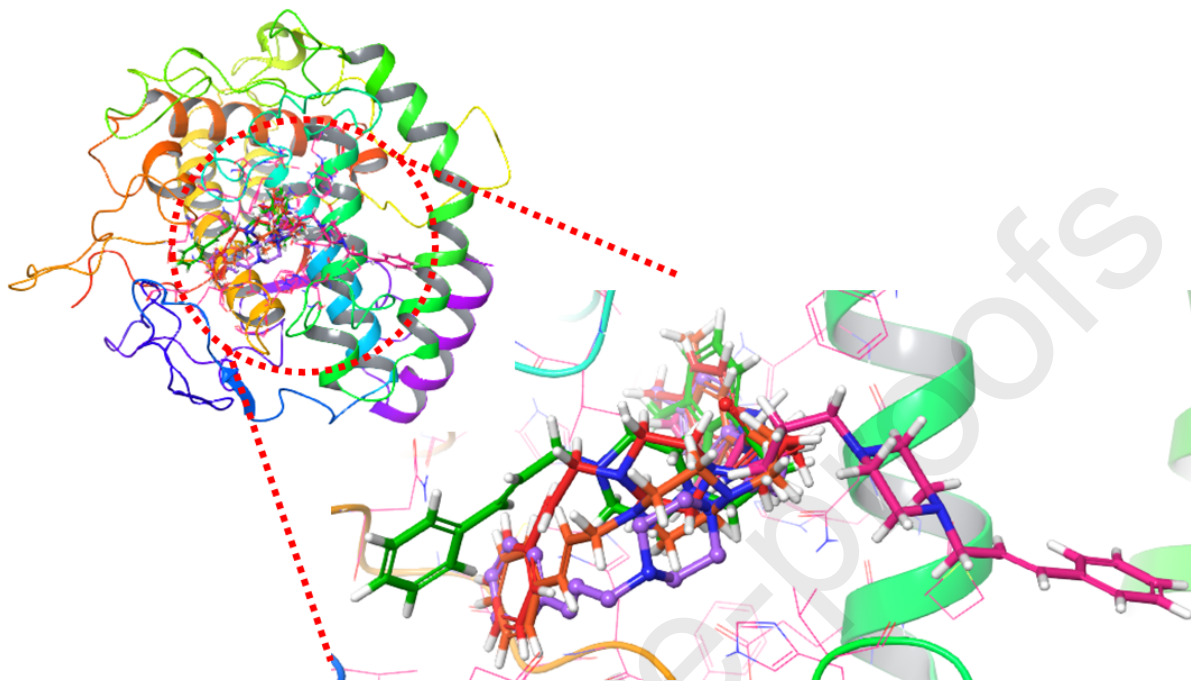


**Fig 3.** Docking complex of **5a-e** within the active region of target protein along with binding energy values (kcal/mol).

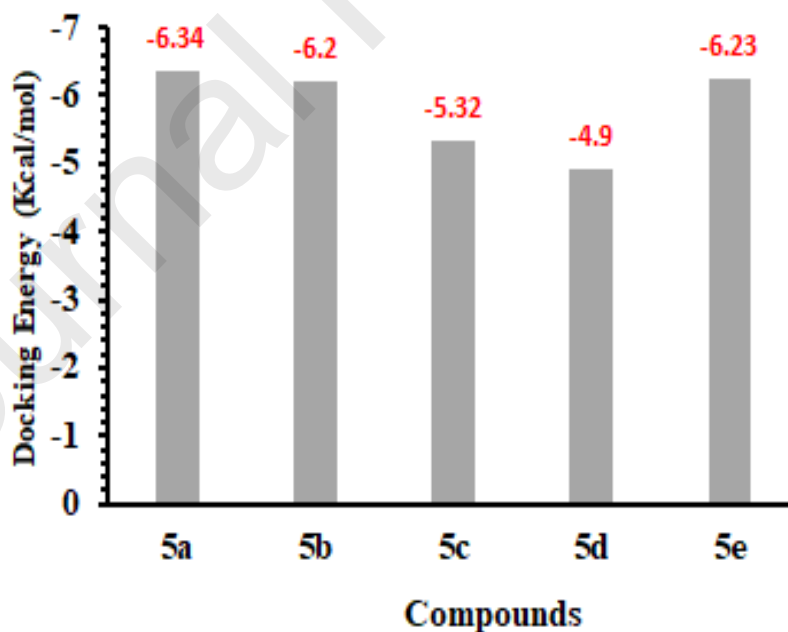


**Figure 4.** Docking complex of **5a-e** within the active region of target protein along with binding energy values (kcal/mol).

### 2.2.5.2. Binding analysis of ligands against tyrosinase

Based on *in vitro* results, the **5b**-docking complex was evaluated to understand their binding conformational analysis within the active site of the target protein. In detail, *in silico* docking analysis revealed that three  $\pi$ - $\pi$  interactions were observed in the **5b**-docking complex. The 3D and 2D depictions of most active compounds **5b** has been mentioned in Fig. 5 A, B. The benzene ring formed  $\pi$ - $\pi$  interaction with His85, whereas, the other two interactions were observed at aromatic residues His259 and His263.

Literature data also ensured the importance of these residues in bonding with other tyrosinase inhibitors which strengthened our docking results [16-18].

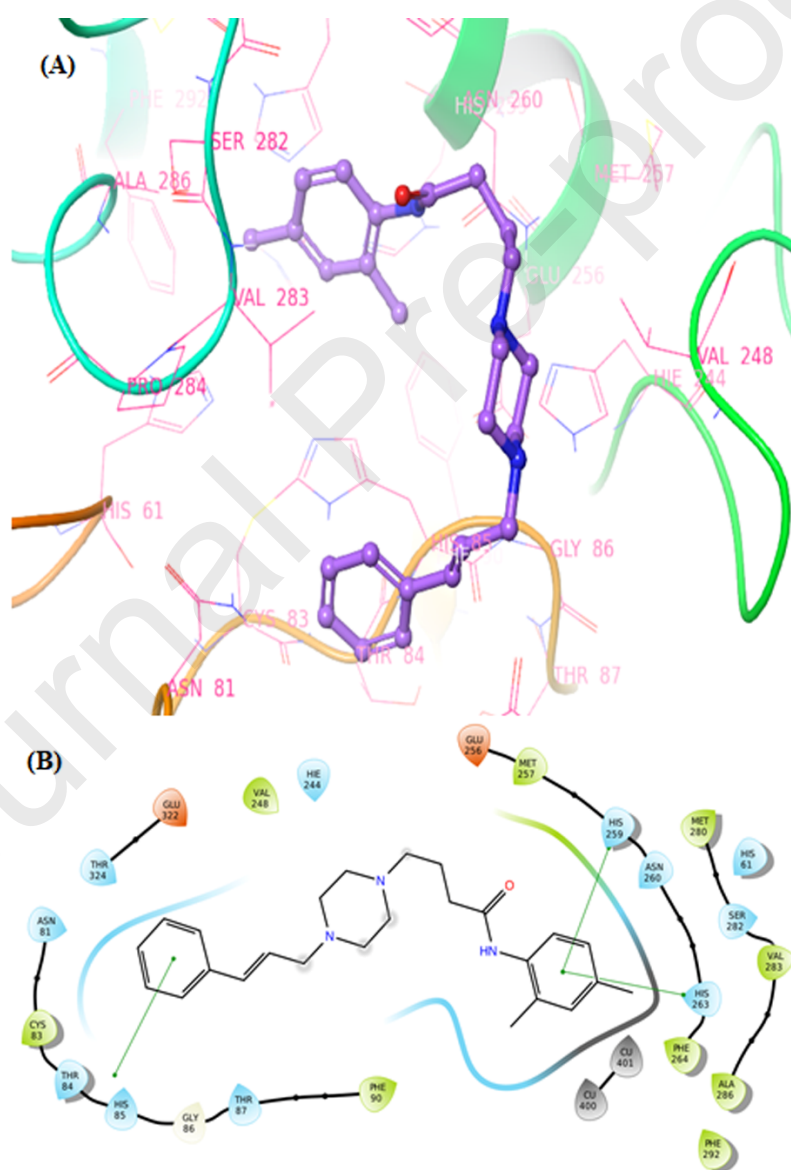


**Figure 5 (A and B).** 3D and 2D docking depictions of **5b** complex against tyrosinase.

## 2.2.6. Molecular dynamic simulations

### 2.2.6.1. Root mean square deviation and fluctuation (RMSD/RMSF) analysis

To evaluate the residual flexibility of the receptor (c-alpha and backbone) through MD simulation RMSD graph was generated to evaluate the protein structural behavior. The RMSD is used to measure the average change in displacement of a selection of atoms for a particular frame with respect to a reference frame. The RMSD graph result of **5b** interprets the protein residual deviation in a 100 ns simulation time frame. Initially, the graph line showed an increasing trend from 0-40 ns having an RMSD value range from 1.00 and 1.75 Å for backbone residues. The generated RMSD graph showed little stability with fluctuations from 40 to 60 ns having RMSD value range from 1.75 -2.00 Å. A Similar trend was observed from 60-100 ns with fluctuations. The overall RMSD analysis showed that fluctuations in the graph in the whole simulation are within the standard range of RMSD 1-2.25 Å which showed backbone stability in docking (Fig. 6). The RMSF is useful for characterizing local changes along with the protein structure. The generated plot indicated protein behavior fluctuations during the simulation in C $\alpha$  and backbone residues. The overall results showed that N- and C-terminals loop regions showed little fluctuations whereas, residues around 170-200 depicted high fluctuations in 100 ns simulation (Fig. 7).

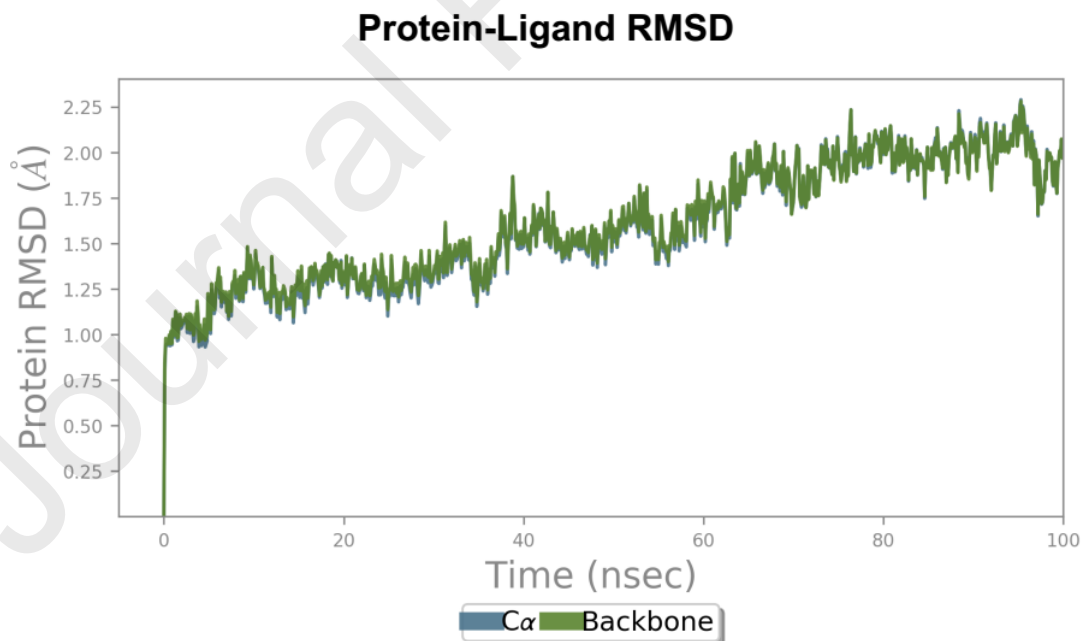


**Figure 6.** RMSD graph of **5b** docking complex at 100 ns.

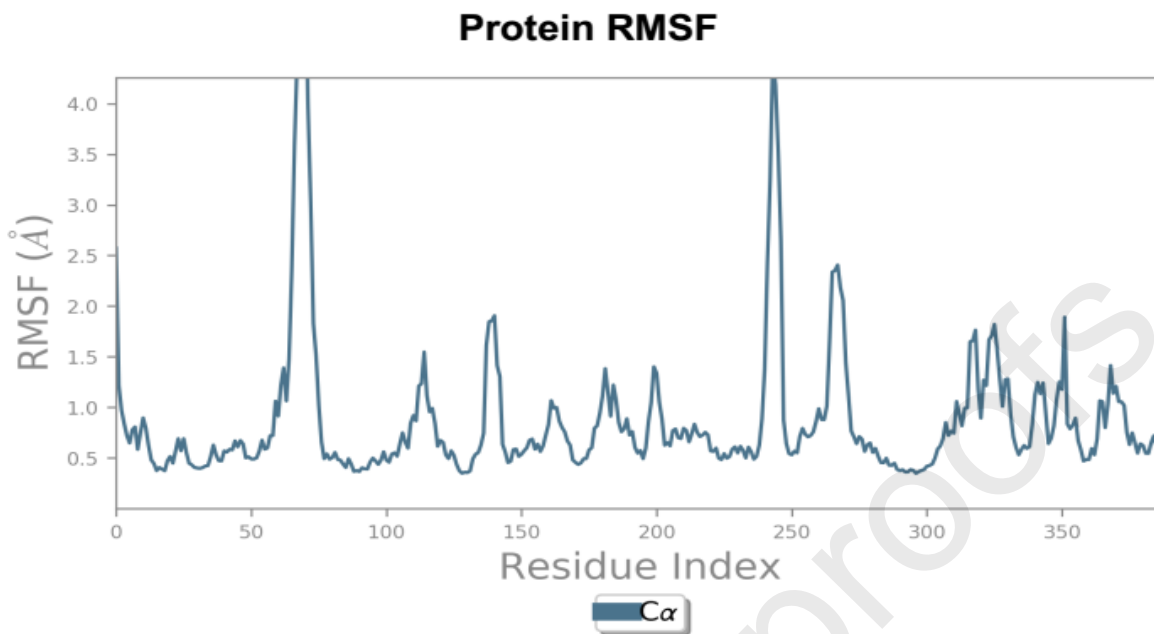


**Figure 7.** RMSF graph of **5b** docking complex at 100 ns.

### 3. Conclusion

A structurally unique series of *N*-(substituted-phenyl)-4-{{4-[(*E*)-3-phenyl-2-propenyl]-1 piperaziny}butanamides (**5a-e**) was synthesized successfully and their structural characterization was carried through spectral analysis lucidly. The title compounds were screened for their mushroom tyrosinase inhibitory activity, compound **5b** showed excellent activity with  $0.013 \pm 0.001 \mu\text{M}$  while  $\text{IC}_{50}$  value of standard kojic acid is  $16.841 \pm 1.146 \mu\text{M}$ . The computational molecular docking performed against tyrosinase protein (PDB ID: 2Y9X) showed that **5b** which is bound in active binding site of the protein. The molecular modeling demonstrates that the oxygen atom of the compound **5b** synchronized with the key residues in the energetic site of the enzyme. Zebrafish result showed the **5b** significantly reduced the pigment without harming the zebrafish. Most of the compounds also displayed mild cytotoxicity. The compound **5a** also exhibited promising results. These results revealed that compounds **5b** and **5a** could be the lead chemical entities in developing the most potent tyrosinase inhibitors for the removal of extra pigment from humans and the prevention of browning in fruits with modest cytotoxicity.

### 4. Experimental

#### 4.1. Chemistry

##### 4.1.1. Materials and method

All the chemicals, along with analytical grade solvents, were purchased from Sigma Aldrich, Alfa Aesar (Germany), or Merck through local suppliers. Pre-coated silica gel Al-plates were used for TLC with ethyl acetate and *n*-hexane as solvent system. Spots were detected by UV<sub>254</sub>. Gallenkamp apparatus was used to detect melting points in capillary tubes. IR spectra ( $\nu$ ,  $\text{cm}^{-1}$ ) were recorded by the KBr pellet method in the Jasco-320-A spectrophotometer. <sup>1</sup>H-NMR spectra ( $\delta$ , ppm) were recorded at 600 MHz (<sup>13</sup>C-NMR spectra, at 150 MHz) in CDCl<sub>3</sub> using the Bruker Advance III 600 As- cend spectrometer using BBO probe. The <sup>1</sup>H-NMR spectral peaks for interpretation are abbreviated as follows: s, singlet; d, doublet; dd, doublet of doublets; t, triplet; br.t, broad triplet; q, quartet; quint, quintet; sex, sextet; sep, septet; m, multiplet, dist, distorted.

##### 4.1.2. Procedure for the synthesis of 4-Chloro-*N*-(substituted-phenyl)butanamides (**3a-e**)

Substituted aniline (**1a-e**, 8.8 mmol; one in each respective reaction) was suspended in 25 mL distilled water, stirred for 30 minutes followed by the addition of 10% aqueous Na<sub>2</sub>CO<sub>3</sub> to adjust pH to 9-10. Then, equimolar quantity of 4-chlorobutanoyl chloride (**2**, 1 mL, 8.8 mmol) was added with vigorous shaking, and the mixture was then set to stirring further for four to five hours till completion of each respective reaction. Reaction progress was monitored by TLC until single spot was achieved. During work-up, respective products were precipitated by lowering the pH up to 2.0 with conc. HCl. The precipitates of these electrophiles, 4-chloro-*N*-(substituted-phenyl)butanamides (**3a-e**) were filtered out, washed with distilled water, and air-dried.

##### 4.1.3. Procedure for the synthesis of *N*-(substituted-phenyl)-4-{4-[(*E*)-3-phenyl-2-propenyl]-1-piperazinyl}butanamides (**5a-e**)

1-[(*E*)-3-Phenyl-2-propenyl]piperazine (**4**, 0.2 g; 0.98 mmol) was taken in 10 mL acetonitrile along with a pinch of K<sub>2</sub>CO<sub>3</sub>, and the mixture was refluxed for half an hour for activation of this nucleophile. Then, calculated amount of one of the substituted electrophiles (**3a-e**, 0.98 mmol) was added and reaction mixture was again set to reflux further for 4-5 hrs. Reaction completion was monitored by TLC. After completion, the reaction mixture was poured on crushed ice and precipitate of respective product was filtered out, washed and air dried. Thus, pure *N*-(substituted-phenyl)-4-{4-[(*E*)-3-phenyl-2-propenyl]-1-piperazinyl}butanamides (**5a-e**) were obtained, which were used for further studies.

##### 4.1.4. Structural characterization

4.1.4.1. *N*-(2,3-Dimethylphenyl)-4-{4-[(*E*)-3-phenyl-2-propenyl]-1-piperazinyl}butanamide (**5a**)

Brown amorphous powder; Yield 72%; m.p. 104-105 °C; Molecular Formula: C<sub>25</sub>H<sub>33</sub>N<sub>3</sub>O; Molecular Mass: 391 gmol<sup>-1</sup>; IR (KBr, ν, cm<sup>-1</sup>): 3249 (N-H, str.), 3047 (Ar C-H str.), 1715 (C=O, str.), 1630 (Ar C=C, str.), 1586 (C=C, str.); <sup>1</sup>H-NMR (CDCl<sub>3</sub>, 600 MHz, δ, ppm): 9.29 (s, 1H, -NH-CO), 7.44 (br.d, *J* = 7.4 Hz, 2H, H-2''' & H-6'''), 7.32 (br.t, *J* = 7.4 Hz, 2H, H-3''' & H-5'''), 7.23 (dist.t, *J* = 7.2 Hz, 1H, H-4'''), 7.11 (br.d, *J* = 7.6 Hz, 1H, H-6'''), 7.03 (br.t, *J* = 7.4 Hz, 1H, H-5'''), 6.99 (br.d, *J* = 7.26 Hz, 1H, H-4'''), 6.53 (br.d, *J* = 15.9 Hz, 1H, H-3''), 6.29 (td, *J* = 6.5, 15.9 Hz, 1H, H-2''), 3.45-3.44 (m, 4H, CH<sub>2</sub>-3' & CH<sub>2</sub>-5'), 3.09 (br.d, *J* = 6.18 Hz, 2H, CH<sub>2</sub>-1''), 2.48-2.46 (m, 2H, CH<sub>2</sub>-4), 2.36-2.28 (m, 6H, CH<sub>2</sub>-2, CH<sub>2</sub>-2' & CH<sub>2</sub>-6'), 2.24 (s, 3H, 3''''-CH<sub>3</sub>), 2.05 (s, 3H, 2''''-CH<sub>3</sub>), 1.74 (quint. *J* = 6.9 Hz, 2H, CH<sub>2</sub>-3); <sup>13</sup>C-NMR (150 MHz, CDCl<sub>3</sub>, δ, ppm): 171.49 (-NH-CO), 137.22 (C-1'''), 137.17 (C-1'''), 132.72 (C-3'''), 132.36 (C-2''), 129.01 (C-3''' & C-5'''), 127.81 (C-4'''), 127.66 (C-4'''), 127.18 (C-5'''), 126.67 (C-2'''), 126.63 (C-2''' & C-6'''), 125.50 (C-3''), 124.10 (C-6'''), 60.65 (C-1''), 57.84 (C-4), 53.22 (C-3' & C-5'), 53.20 (C-2' & C-6'), 34.17 (C-2), 23.04 (C-3), 20.58 (C-3'''), 14.46 (C-2'''); Anal. Calc. for C<sub>25</sub>H<sub>33</sub>N<sub>3</sub>O (391.55): C, 76.61; H, 8.42; N, 10.70. Found: C, 76.59; H, 8.40; N, 10.68.

4.1.4.2. *N*-(2,4-Dimethylphenyl)-4-{4-[(*E*)-3-phenyl-2-propenyl]-1-piperazinyl}butanamide (**5b**)

Dark brown solid; Yield 85%; m.p. 121-122 °C; Molecular Formula: C<sub>25</sub>H<sub>33</sub>N<sub>3</sub>O; Molecular Mass: 391 gmol<sup>-1</sup>; IR (KBr, ν, cm<sup>-1</sup>): 3251 (N-H, str.), 3043 (Ar C-H, str.), 1717 (C=O, str.), 1635 (Ar C=C, str.), 1590 (C=C, str.); <sup>1</sup>H-NMR (CDCl<sub>3</sub>, 600 MHz, δ, ppm): 9.14 (s, 1H, -NH-CO), 7.44 (br.d, *J* = 7.4 Hz, 2H, H-2''' & H-6'''), 7.32 (br.t, *J* = 7.5 Hz, 2H, H-3''' & H-5'''), 7.23 (br.t, *J* = 7.4 Hz, 1H, H-4'''), 7.21 (br.d, *J* = 7.9 Hz, 1H, H-6'''), 7.00 (br.s, 1H, H-3'''), 6.94 (br.d, *J* = 7.7 Hz, 1H, H-5'''), 6.53 (br.d, *J* = 15.9 Hz, 1H, H-3''), 6.29 (td, *J* = 6.6, 15.9 Hz, 1H, H-2''), 3.38-3.34 (m, 4H, CH<sub>2</sub>-3' & CH<sub>2</sub>-5'), 3.09 (br.d, *J* = 6.4 Hz, 2H, CH<sub>2</sub>-1''), 2.48-2.46 (m, 2H, CH<sub>2</sub>-4), 2.39-2.30 (m, 6H, CH<sub>2</sub>-2, CH<sub>2</sub>-2' & CH<sub>2</sub>-6'), 2.24 (s, 3H, 4''''-CH<sub>3</sub>), 2.14 (s, 3H, 2''''-CH<sub>3</sub>), 1.73 (quint. *J* = 7.14 Hz, 2H, CH<sub>2</sub>-3); <sup>13</sup>C-NMR (150 MHz, CDCl<sub>3</sub>, δ, ppm): 171.42 (NH-CO), 137.16 (C-1'''), 137.17 (C-1'''), 134.47 (C-1'''), 134.46 (C-2'''), 132.37 (C-2''), 132.17 (C-4'''), 131.15 (C-5'''), 129.01 (C-3''' & C-5'''), 127.81 (C-3'''), 127.64 (C-4'''), 126.77 (C-6'''), 126.63 (C-2''' & C-6'''), 125.69 (C-3''), 60.65 (C-1''), 57.84 (C-4), 53.28 (C-3' & C-5'), 53.19 (C-2' & C-6'), 34.20 (C-

2), 23.04 (C-3), 20.91 (C-4'''), 18.23 (C-2'''); Anal. Calc. for C<sub>25</sub>H<sub>33</sub>N<sub>3</sub>O (391.55): C, 76.61; H, 8.42; N, 10.70. Found: C, 76.62; H, 8.41; N, 10.71.

4.1.4.3. *N*-(3-Methylphenyl)-4-{(4-[(*E*)-3-phenyl-2-propenyl]-1-piperazinyl}butanamide  
(5c)

Pink amorphous semi-solid, Molecular Formula: C<sub>24</sub>H<sub>31</sub>N<sub>3</sub>O; Molecular Mass: 377 gmol<sup>-1</sup>; IR (KBr, ν, cm<sup>-1</sup>): 3256 (N-H, str.), 3047 (Ar C-H, str.), 1713 (C=O, str.), 1630 (Ar C=C, str.), 1588 (C=C, str.); <sup>1</sup>H-NMR (CDCl<sub>3</sub>, 600 MHz, δ, ppm): 9.77 (s, 1H, NH-CO), 7.43 (br.d, *J* = 7.26 Hz, 2H, H-2''' & H-6'''), 7.37 (br.d, *J* = 8.4 Hz, 1H, H-6'''), 7.32 (dist.t, *J* = 7.8 Hz, 2H, H-3''' & H-5'''), 7.24 (m, 1H, H-4'''), 7.15 (br.t, *J* = 7.8 Hz, 1H, H-5'''), 6.84 (br.d, *J* = 7.3 Hz, 1H, H-4'''), 6.54 (br.d, *J* = 15.9 Hz, 1H, H-3''), 6.50 (dist.d, *J* = 3.2 Hz, 1H, H-2'''), 6.29 (td, *J* = 6.5, 15.9 Hz, 1H, H-2''), 3.45-3.43 (m, 4H, CH<sub>2</sub>-3' & CH<sub>2</sub>-5'), 3.07 (dist.d, *J* = 6.5 Hz, 2H, CH<sub>2</sub>-1''), 2.43-2.39 (m, 2H, CH<sub>2</sub>-4), 2.37-2.34 (m, 6H, CH<sub>2</sub>-2, CH<sub>2</sub>-2' & CH<sub>2</sub>-6'), 2.21 (s, 3H, 3'''-CH<sub>3</sub>), 1.73 (quint., *J* = 7.1 Hz, 2H, CH<sub>2</sub>-3); <sup>13</sup>C-NMR (150 MHz, CDCl<sub>3</sub>, δ, ppm): 171.52 (NH-CO), 139.77 (C-1'''), 138.66 (C-3'''), 137.16 (C-1'''), 132.37 (C-2''), 129.00 (C-3''' & C-5'''), 128.87 (C-5'''), 127.88 (C-4'''), 127.80 (C-3''), 127.63 (C-4'''), 127.17 (C-2'''), 126.62 (C-2''' & C-6'''), 120.13 (C-6'''), 60.64 (C-1''), 57.78 (C-4), 53.25 (C-3' & C-5'), 53.20 (C-2' & C-6'), 34.87 (C-2), 22.79 (C-3), 21.65 (C-3'''); Anal. Calc. for C<sub>24</sub>H<sub>31</sub>N<sub>3</sub>O (377.52): C, 76.28; H, 8.21; N, 11.12. Found: C, 76.29; H, 8.22; N, 11.10.

4.1.4.4. *N*-(4-Methylphenyl)-4-{(4-[(*E*)-3-phenyl-2-propenyl]-1-piperazinyl}butanamide  
(5d)

Dark brown semi-solid; Yield 80%; Molecular Formula: C<sub>24</sub>H<sub>31</sub>N<sub>3</sub>O; Molecular Mass: 377 gmol<sup>-1</sup>; IR (KBr, ν, cm<sup>-1</sup>): 3253 (N-H, str.), 3049 (Ar C-H, str.), 1719 (C=O, str.), 1633 (Ar C=C, str.), 1594 (C=C, str.); <sup>1</sup>H-NMR (CDCl<sub>3</sub>, 600 MHz, δ, ppm): 9.75 (s, 1H, NH-CO), 7.47 (br.d, *J* = 8.2 Hz, 2H, H-2''' & H-6'''), 7.43 (br.d, *J* = 7.3 Hz, 2H, H-2''' & H-6'''), 7.32 (dist.t, *J* = 7.5 Hz, 2H, H-3''' & H-5'''), 7.23 (dist.t, *J* = 7.3 Hz, 1H, H-4'''), 7.08 (br.d, *J* = 8.2 Hz, 2H, H-3''' & H-5'''), 6.51 (br.d, *J* = 15.9 Hz, 1H, H-3''), 6.28 (td, *J* = 6.4, 15.9 Hz, 1H, H-2''), 3.45-3.44 (m, 4H, CH<sub>2</sub>-3' & CH<sub>2</sub>-5'), 3.06 (br.d, *J* = 6.4 Hz, 2H, CH<sub>2</sub>-1''), 2.46-2.43 (m, 2H, CH<sub>2</sub>-4), 2.34-2.27 (m, 6H, CH<sub>2</sub>-2, CH<sub>2</sub>-2' & CH<sub>2</sub>-6'), 2.24 (s, 3H, 4'''-CH<sub>3</sub>), 1.72 (quint. *J* = 7.1 Hz, 2H, CH<sub>2</sub>-3); <sup>13</sup>C-NMR (150 MHz, CDCl<sub>3</sub>, δ, ppm): 171.35 (NH-CO), 137.33 (C-1'''), 137.16 (C-1'''), 132.73 (C-4'''), 132.35 (C-2''), 129.41 (C-3''' & C-5'''), 129.00 (C-3''' & C-5'''), 127.65 (C-4'''), 126.66 (C-3''), 126.62 (C-2''' & C-6'''), 119.55 (C-2''' & C-6'''), 60.64 (C-1''), 57.80 (C-4), 53.26 (C-3' & C-5'), 53.22 (C-2' &

C-6'), 34.81 (C-2), 22.81 (C-3), 20.87 (C-4'''); Anal. Calc. for C<sub>24</sub>H<sub>31</sub>N<sub>3</sub>O (377.52): C, 76.28; H, 8.21; N, 11.12. Found: C, 76.26; H, 8.24; N, 11.14.

4.1.4.5. *N*-(4-Ethylphenyl)-4-{4-[(*E*)-3-phenyl-2-propenyl]-1-piperazinyl}butanamide  
(5e)

Light pink amorphous powder; Yield 71%; m.p. 125-126 °C; Molecular Formula: C<sub>25</sub>H<sub>33</sub>N<sub>3</sub>O; Molecular Mass: 391 gmol<sup>-1</sup>; IR (KBr,  $\nu$ , cm<sup>-1</sup>): 3243 (N-H, str.), 3047 (Ar C-H, str.), 1711 (C=O, str.), 1635 (Ar C=C, str.), 1592 (C=C, str.); <sup>1</sup>H-NMR (CDCl<sub>3</sub>, 600 MHz,  $\delta$ , ppm): 9.23 (s, 1H, NH-CO), 7.44 (br.d,  $J$  = 7.5 Hz 2H, H-2''' & H-6'''), 7.33-7.31 (m, 3H, H-3''', H-4''' & H-5'''), 7.22 (br.d,  $J$  = 8.0 Hz, 2H, H-2'''' & H-6'''), 7.12 (br.d,  $J$  = 8.0 Hz, 2H, H-3'''' & H-5'''), 6.53 (br.d,  $J$  = 15.9 Hz, 1H, H-3''), 6.29 (td,  $J$  = 6.6, 15.9 Hz, 1H, H-2''), 3.38-3.34 (m, 4H, CH<sub>2</sub>-3' & CH<sub>2</sub>-5'), 3.09 (br.d,  $J$  = 6.3 Hz, 2H, CH<sub>2</sub>-1''), 2.58 (q,  $J$  = 7.5 Hz, 2H, 4''''-CH<sub>2</sub>CH<sub>3</sub>), 2.48-2.47 (m, 2H, CH<sub>2</sub>-4), 2.33-2.25 (m, 6H, CH<sub>2</sub>-2, CH<sub>2</sub>-2' & CH<sub>2</sub>-6'), 1.74 (quint.,  $J$  = 7.1 Hz, 2H, CH<sub>2</sub>-3) 1.11 (t,  $J$  = 7.5 Hz, 3H, 4''''-CH<sub>2</sub>CH<sub>3</sub>); <sup>13</sup>C-NMR (150 MHz, CDCl<sub>3</sub>,  $\delta$ , ppm): 171.76 (NH-CO), 138.42 (C-1'''), 137.16 (C-1'''), 136.26 (C-4'''), 132.36 (C-2''), 129.01 (C-3''' & C-5'''), 128.86 (C-3'''' & C-5'''), 127.81 (C-2'''' & C-6'''), 127.65 (C-4'''), 126.58 (C-2''' & C-6'''), 126.25 (C-3''), 60.65 (C-1''), 57.81 (C-4), 53.29 (C-3' & C-5'), 53.20 (C-2' & C-6'), 34.17 (C-2), 24.23 (4''''-CH<sub>2</sub>CH<sub>3</sub>), 23.01 (C-3) 14.68 (4''''-CH<sub>2</sub>CH<sub>3</sub>); Anal. Calc. for C<sub>25</sub>H<sub>33</sub>N<sub>3</sub>O (391.55): C, 76.61; H, 8.42; N, 10.70. Found: C, 76.60; H, 8.44; N, 10.72.

## 4.2. Biology

### 4.2.1. In vitro methodology

#### 4.2.1.1. Tyrosinase assay

The potency of synthesized amides against tyrosinase was investigated by exactly following our published method [19,20]. In the first step, 20 mM with pH 6.8 Phosphate buffer was prepared and their 140  $\mu$ L was used in each well, simultaneously 20  $\mu$ L of target enzyme mushroom tyrosinase was also added from 30U/mL of stock solution. In a third step, 20  $\mu$ L of the compound was poured into the assay plate. After the first incubation of 10 minutes at 25 °C, the 20  $\mu$ L of substrate L\_DOPA was poured from a stock solution of 0.85 mM, after that reaction mixture was again incubated 20 minutes at room temperature. Finally, the change in absorbance was recorded at wavelength 475 nm using SpectraMAX ABS microplate reader. For comparison and assay validation kojic acid was used as positive control and assay buffer was used as a negative control. For IC<sub>50</sub> calculations all concentration was investigated separately and repeated three

times for better accuracy of results. For calculation of IC<sub>50</sub> through nonlinear regression GraphPad Prism was used. By below mentioned equation % inhibition was determined.

$$\text{Tyrosinase \% inhibition} = \frac{(\text{Blank} - \text{Sample})}{\text{Blank}} \times 100$$

#### 4.2.1.2. Kinetic analysis

The kinetic experiment was carried to know the behavior of compound **5b** for inhibition of tyrosinase. Range of doses was investigated for the identification of the pattern of inhibition of tyrosinase by **5b** we examined the kinetic using our published method [20]. Totally four doses of **5b** were investigated 0.00, 0.007, 0.013 and 0.026  $\mu\text{M}$ . various series of substrate L-DOPA doses were used from 0.0625 to 2mM for all experiments. The first incubation and reading period was the same as presented in the above inhibition method for IC<sub>50</sub> calculations. The maximum first velocity was determined using the primary linear phase of absorbance for 5 minutes after mixing enzyme solution at thirty seconds period. The enzyme blockage pattern was determined using the Lineweaver Burk graph of the opposite of velocities (1/V) against the opposite of used substrate doses. Another chart was drawn for calculations of enzyme inhibition dissociation constant *K<sub>i</sub>* through 1/V against the **5b** doses.

#### 4.2.1.3. Hemolytic activity

For a hemolytic activity study, the bovine blood sample was collected in EDTA, diluted with (0.9% NaCl), and centrifuge the diluted sample at 1000xg for 10 minutes. The erythrocytes separated, diluted in phosphate buffer of pH 7.4, and suspension was made. 20  $\mu\text{L}$  of synthesized compounds solution (10 mg/mL) in 180  $\mu\text{L}$  of RBCs suspension was added and then incubated for 30 min at room temperature. PBS was used as negative control and Triton-X was taken as a positive control [21,22]. The experiment was performed in triplicate. The %age of hemolytic activity (cytotoxicity) of newly synthesized amides was calculated by using the following formula:

$$(\%) \text{ of Hemolysis} = \frac{\text{Absorbance of Sample} - \text{Absorbance of Negative Control}}{\text{Absorbance of Positive Control}} \times 100$$

#### 4.2.2. In vivo methodology

##### 4.2.2.1. Determination of pigmentation reducing capacity of **5b** in embryos of Zebrafish

The animal experiments were carried out as accordance with the published methods [20,23].

#### 4.2.2.2. *Zebrafish Farming*

The selected animal zebrafishes were obtained from the local market and maintained in our fish facility laboratory for thirty days. All the conditions were optimized for fish culture as prescribed in literature for zebrafish maintains. Shrimp larvae were used as the food of fishes and they were housed in tanks made up of thermostatic material. For respiration, growth and better health air and water filtration were maintained. The fish seed was obtained using the normal procedure of fish spawning performed using the light source as a stimulator. All the animal experiments methods were confirmed by the Departmental Review Board on Kongju National University (IRB NO. 2011-2).

#### 4.2.2.3. *Compound 5b treatment and depigmentation examination*

Firstly the E3 medium was prepared by mixing the 5mM Sodium chloride, 0.17mM of potassium chloride, 0.33mM calcium chloride and 0.33 mM and magnesium chloride. After that even fishes were obtained using pipette into an assay plate and poured four to five embryos in each well. In the second step, **5b** solution was prepared in 0.1% DMSO and placed into the embryos medium for nine to seventy-two hours post-fertilization. For comparison and assay confirmation kojic acid was used as a reference. After that chorion of embryos was removed and tricainemethanesulfonate MS-222 was used as anesthesia. Lastly, embryos slide was prepared using 1% methylcellulose on the whole slide and images were takes using stereomicroscope purchased from Nikon, Japan.

#### 4.2.3. *Computational Methodology*

##### 4.2.3.1. *Grid generation and molecular docking*

The three dimensional (3D) structure of mushroom tyrosinase (*Agaricus bisporus*) (PDB ID: 2Y9X) was accessed from the Protein Data Bank (PDB). Before the molecular docking experiment, we modified the target protein structure for better docking results. The tyrosinase structure was prepared by using the "Protein Preparation Wizard" by the Maestro interface in Schrödinger Suite. Initially, bond orders were assigned and hydrogen atoms were added to the protein structure. After that, the structure was then minimized to reach the converged root mean square deviation (RMSD) of 0.30 Å with the OPLS\_2005 force field. The active site of the enzyme (tyrosinase) was defined from the co-crystallized ligands from PDB and literature data [16-18]. The synthesized ligands (**5a-e**) were sketched in a 2D sketcher in Schrödinger Suite and saved in the Maestro interface for docking experiments. The molecular docking experiment was performed

for all the synthesized ligands against target protein by using a Glide docking protocol [24]. The predicted binding energies (docking scores) and conformational positions of ligands within the active region of protein were also performed using the Glide experiment. Throughout the docking simulations, both partial flexibility and full flexibility around the active site residues are performed by Glide/SP/XP and induced fit docking (IFD) approaches [25].

#### 4.2.3.2. *Molecular Dynamics*

To understand the protein backbone stability in docking complex (**5b**), a molecular dynamics simulation experiment was carried out using the Desmond simulation package of Schrödinger [26]. In all runs, the NPT (isothermal-isobaric) ensemble was applied with a temperature of 300 K and pressure of 1 bar. The simulation length was 100 ns, with relaxation time 1 ps. The force field parameters for each simulation were according to OPLS\_2005 [27]. The long-range electrostatic interactions were calculated using the particle mesh Ewald (PME) method [28]. The cutoff radius in Coulomb interactions was 9.0 Å. The water molecules were described using a simple point charge model (SPC) [29]. The Martyna-Tuckerman-Klein chain coupling scheme [30] with a coupling constant of 2.0 ps was used for pressure control and the Nosé-Hoover chain coupling scheme for temperature control. Non bonded forces were calculated using an r-RESPA integrator, where the short-range forces were updated every step and the long-range forces were updated every 3 steps. The trajectories were saved at 4.8 ps intervals for analysis. To analyze the behavior and interactions between the ligands and protein, we used the Simulation Interactions Diagram tool implemented in the Desmond molecular dynamics package.

#### **Acknowledgement**

The present study was supported by Basic Science Research Program through the National Research Foundation of Korea (NRF) funded by the Ministry of Education (2017R1D1A1B03034948).

#### **Declaration of Competing Interest**

The authors declare no conflict of interests.

#### **Authors Contribution**

<sup>a</sup> *College of Natural Science, Department of Biological Sciences, Kongju National University, Gongju, 32588, South Korea.*

The study designed, animal, tyrosinase screening were performed, manuscript was completed for finalized submission.

<sup>b</sup> *Department of Chemistry, Government College University, Lahore-54000, Pakistan.*

Scheme was designed and synthesis of organic compounds were carried out.

<sup>c</sup> *Institute of Molecular Biology and Biotechnology (IMBB), The University of Lahore, Lahore-54000,, Pakistan.*

Molecular docking study was performed.

<sup>d</sup> *Department of Physiology, University of Sindh, Jamshoro Pakistan.*

In silico study and helps in drafting the manuscript.

<sup>e</sup> *Faculty of Pharmacy and Atta-ur-Rahman Institute for Natural Products Discovery (AuRIns), Level 9, FF3, Universiti Teknologi MARA, Puncak Alam Campus, 42300 Bandar Puncak Alam, Selangor Darul Ehsan, Malaysia.*

Characterization of compounds was performed.

<sup>f</sup> *Department of Biochemistry, University of Agriculture, Faisalabad-38040, Pakistan.*

Toxicity was assessed.

## References

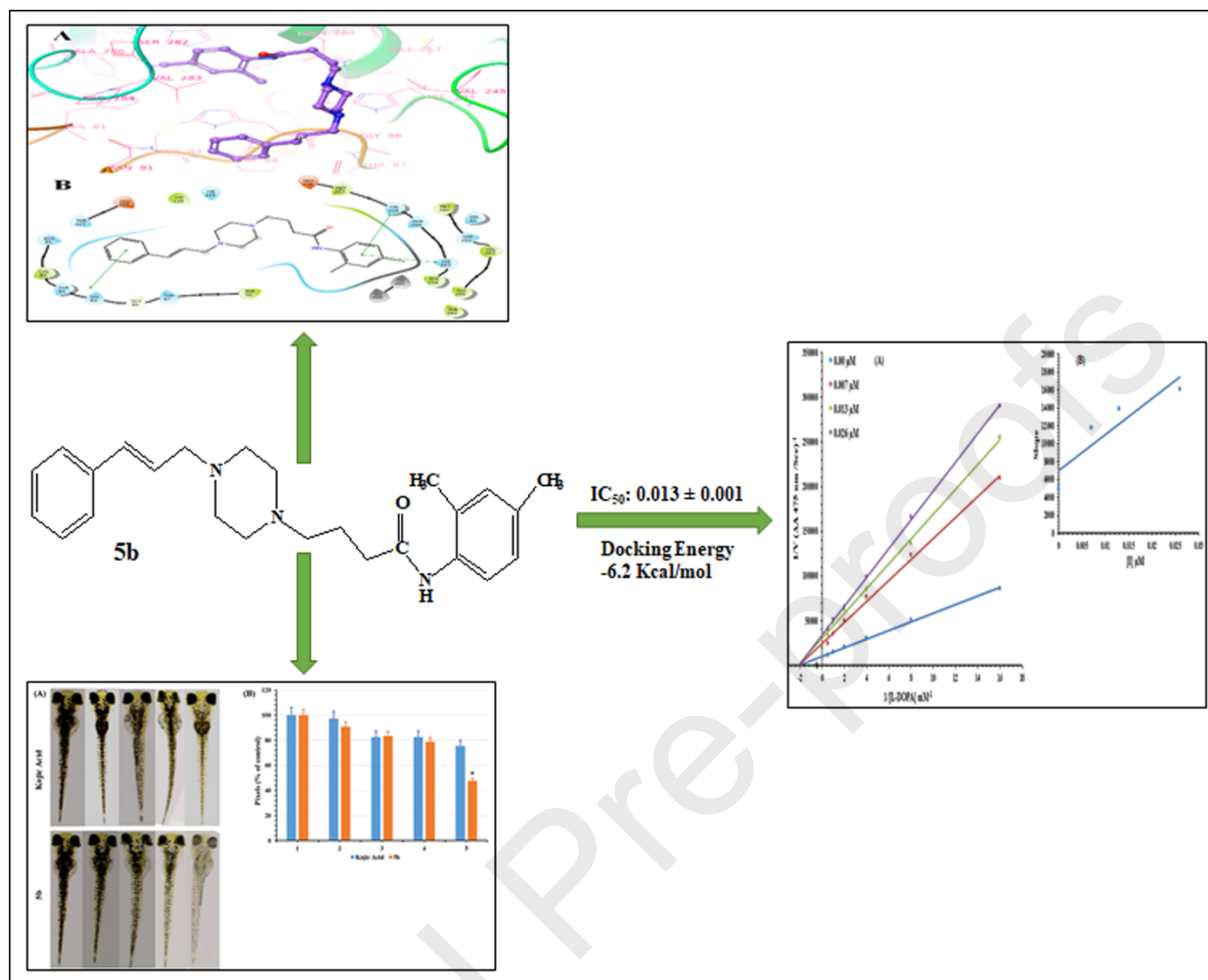
- [1] A. Todorovic, C. Haskell-Luevano, A review of melanocortin receptor small molecule ligands. *Peptides*. 26 (2005) 2026–36.
- [2] Q. Wu, Z.C. Wang, X. Wei, W. Xue, Synthesis and antibacterial activities of 1-substituted-4-[5-(4-substitutedphenyl)-1, 3, 4-thiadiazol-2-sulfonyl] piperazine derivatives, *Chin. J. Synth. Chem.* 22 (2014) 429–434.
- [3] D.H. Jiang, M. Huang, Design and synthesis of thieno [3, 2-d] pyrimidine derivatives containing a piperazine unit as anticancer agents, *Chem. Reag.* 34 (2012) 797–799.
- [4] M.A. Abbasi, A. Anwar, S.Z. Siddiqui, K. Rubab, M.A. Lodhi, F.A. Khan, M. Ashraf, U. Alam, Synthesis, enzyme inhibition and molecular docking studies of 1-Arylsulfonyl-4-phenylpiperazine derivatives, *Pak. J. Pharm. Sci.* 30 (2017) 1715–1724.
- [5] S. Liang, C.M. Liu, Y.S. Jin, Synthesis and antifungal activity of 1-(1H-1, 2, 4-triazol-1-yl)-2-(2, 4-difluorophenyl)-3-[(4-substituted)-p iperazine-1-yl]-2-propanols, *Chin. J. Med. Chem.* 14 (2004) 71–75.
- [6] H. Foks, M. Janowiec, Z. Zwolska, E. Augustynowicz-Kopec, Synthesis and tuberculostatic activity of some 2-piperazinmethylene derivatives 1, 2, 4-triazole-3-thiones, Phosphorus, sulfur, silicon. 180 (2005) 537–543.
- [7] B.L. Wang, L.Y. Zhang, Y.Z. Zhan, Y. Zhang, X. Zhang, L.Z. Wang, Z.M. Li, Synthesis and biological activities of novel 1, 2, 4-triazole thiones and bis (1, 2, 4-triazole thiones) containing phenylpyrazole and piperazine moieties, *J. Fluor. Chem.* 184 (2016) 36–44.
- [8] M.H. Helal, S.Y. Abbas, M.A. Salem, A.A. Farag, Y.A. Ammar, Synthesis and characterization of new types of 2-(6-methoxy-2-naphthyl) propionamide derivatives as potential antibacterial and antifungal agents, *Med. Chem. Res.* 22 (2013) 5598–5609.
- [9] B.L. Wang, Y.X. Shi, S.J. Zhang, Y. Ma, H.X. Wang, L.Y. Zhang, W. Wei, X.H. Liu, Y.H. Li, Z.M. Li, B.J. Li, Syntheses, biological activities and SAR studies of novel carboxamide compounds containing piperazine and arylsulfonyl moieties, *Eur. J. Med. Chem.* 117 (2016) 167–178.
- [10] R. Wang, W.M. Chai, Q. Yang, M.K. Wei, Y. Peng, 2-(4-Fluorophenyl)-quinazolin-4 (3H)-one as a novel tyrosinase inhibitor: synthesis, inhibitory activity, and mechanism, *Bioorg. Med. Chem.* 24 (2016) 4620–4625.

- [11] Q. Abbas, Z. Ashraf, M. Hassan, H. Nadeem, M. Latif, S. Afzal, S.Y. Seo, Development of highly potent melanogenesis inhibitor by in vitro, in vivo and computational studies, *Drug Des. Dev. Therapy* 11 (2017) 2029–2046.
- [12] Z.T. Gür, S. Shekfeh, İ.E. Orhan, Novel Piperazine Amides of Cinnamic Acid Derivatives as Tyrosinase Inhibitors, *LETT. DRUG DES. DISCOV.* 16 (2019) 36–44.
- [13] G. Karakaya, A. Türe, A. Ercan, S. Öncül, M.D. Aytemir, Synthesis, computational molecular docking analysis and effectiveness on tyrosinase inhibition of kojic acid derivatives, *Bioorg. Chem.* 88 (2019) 102950.
- [14] A. Ali, Z. Ashraf, M. Rafiq, A. Kumar, F. Jabeen, G.J. Lee, F. Nazir, M. Ahmed, M. Rhee, E.H. Choi, Novel amide derivatives as potent tyrosinase inhibitors; in-vitro, in-vivo antimelanogenic activity and computational studies, *Med. Chem.* 15 (2019) 715–728.
- [15] M.A. Abbasi, M. Hassan, Aziz-ur-Rehman, S.Z. Siddiqui, G. Hussain, S.A.A. Shah, M. Ashraf, M. Shahid, S.Y. Seo, 2-Furoic piperazide derivatives as promising drug candidates of type 2 diabetes and Alzheimer's diseases: *In vitro* and *in silico* studies, *Comp. Bio. Chem.* 77 (2018) 72–86.
- [16] M. Hassan, Z. Ashraf, Q. Abbas, H. Raza, S.Y. Seo, Exploration of novel human tyrosinase inhibitors by molecular modeling, docking and simulation studies, *INTERDISCIP. SC.* 10 (2018) 68–80.
- [17] A. Saeed, P.A. Mahesar, P.A. Channar, Q. Abbas, F.A. Larik, M. Hassan, H. Raza, S.Y. Seo, Synthesis, molecular docking studies of coumarinyl-pyrazolinyl substituted thiazoles as non-competitive inhibitors of mushroom tyrosinase, *Bioorg. Chem.* 74 (2017) 187–196.
- [18] F.A. Larik, A. Saeed, P.A. Channar, U. Muqadar, Q. Abbas, M. Hassan, S.Y. Seo, M. Bolte, Design, synthesis, kinetic mechanism and molecular docking studies of novel 1-pentanoyl-3-arylthioureas as inhibitors of mushroom tyrosinase and free radical scavengers, *Eur. J. Med. Chem.* 141 (2017) 273–281.
- [19] R. Qamar, A. Saeed, F.A. Larik, Q. Abbas, M. Hassan, H. Raza, S.Y. Seo, Novel 1, 3-oxazine-tetrazole hybrids as mushroom tyrosinase inhibitors and free radical scavengers: Synthesis, kinetic mechanism, and molecular docking studies. *Chem. Biol. Drug Des.* 93 (2019) 123–131.

- [20] Q. Abbas, H. Raza, M. Hassan, A.R. Phull, S.J. Kim, S.Y. Seo, Acetazolamide inhibits the level of tyrosinase and melanin: an enzyme kinetic, in vitro, in vivo and in silico studies, *Chem. Biodivers.* 14 (2017) e1700117.
- [21] P. Sharma, J.D. Sharma, In vitro hemolysis of human erythrocytes—by plant extracts with antiplasmodial activity, *J. Ethnopharmacol.* 74 (2001) 239–243.
- [22] M.A. Abbasi, W. Khan, Aziz-ur-Rehman, S.Z. Siddiqui, G. Hussain, S.A.A. Shah, M. Shahid, K.M. Khan, Linear synthesis of {4-[(2-alkoxy/aralkyloxy-3,5-dichlorophenyl)sulfonyl]-1-piperazinyl}(2-furyl)methanones as possible therapeutic agents, *J. Chem. Soc. Pak.* 41 (2019) 685–694.
- [23] T.Y. Choi, J.H. Kim, D.H. Ko, C.H. Kim, J.S. Hwang, S. Ahn, S.Y. Kim, C.D. Kim, J.H. Lee, T.J. Yoon, Zebrafish as a new model for phenotype-based screening of melanogenic regulatory compounds. *Pigment cell Res.* 20 (2007) 120–127.
- [24] R.A. Friesner, R.B. Murphy, M.P. Repasky, L.L. Frye, J.R. Greenwood, T.A. Halgren, P.C. Sanschagrin, D.T. Mainz, Extra precision glide: docking and scoring incorporating a model of hydrophobic enclosure for protein-ligand complexes, *J. Med. Chem.* 49 (2006) 6177–6196.
- [25] R. Farid, T. Day, R.A. Friesner, R.A. Pearlstein, New insights about HERG blockade obtained from protein modeling, potential energy mapping, and docking studies, *Bioorg. Med. Chem.* 14 (2006) 3160–3173.
- [26] K.J. Bowers, D.E. Chow, H. Xu, R.O. Dror, M.P. Eastwood, B.A. Gregersen, J.L. Klepeis, I. Kolossvary, M.A. Moraes, F.D. Sacerdoti, J.K. Salmon, Scalable algorithms for molecular dynamics simulations on commodity clusters, *InSC'06: Proceedings of the 2006 ACM/IEEE Conference on Supercomputing (2006)* (pp. 43–43). IEEE.
- [27] J.L. Banks, H.S. Beard, Y. Cao, A.E. Cho, W. Damm, R. Farid, A.K. Felts, T.A. Halgren, D.T. Mainz, J.R. Maple, R. Murphy, Integrated modeling program, applied chemical theory (IMPACT), *J. Comput. Chem.* 26 (2005) 1752–1780.
- [28] A.Y. Toukmaji, J.A. Board, Ewald summation techniques in perspective: a survey, *Comput. Phys. Commun.* 95 (1996) 73–92.
- [29] J. Zielkiewicz, Structural properties of water: Comparison of the SPC, SPCE, TIP4P, and TIP5P models of water, *J. Chem. Phys.* 123 (2005) 104501.
- [30] G.J. Martyna, M.L. Klein, M. Tuckerman, Nosé–Hoover chains: The canonical ensemble via continuous dynamics, *J. Chem. Phys.* 97 (1992) 2635–2643.

**Highlights**

- Butanamides compounds were synthesized for the treatment of melanogenesis.
- The inhibitory activity of synthesized compounds were evaluated against tyrosinase.
- The compounds were evaluated as an antimelanogenesis using zebrafish.
- The cytotoxicity of these butanamides was also screened using hemolytic activity.
- In silico study was performed to check the binding profile against tyrosinase.



**Declaration of interests**

The authors declare that they have no known competing financial interests or personal relationships that could have appeared to influence the work reported in this paper.

The authors declare the following financial interests/personal relationships which may be considered as potential competing interests:

Journal Pre-proofs